Multiple-scattering effects in Ga K-edge extended x-ray absorption fine structure spectra of GaP, GaAs and GaSb semiconductor compounds

2005 J. Phys.: Condens. Matter 17 8017

(http://iopscience.iop.org/0953-8984/17/50/019)

INSTITUTE OF PHYSICS PUBLISHING JOURNAL OF PHYSICS: CONDENSED MATTER

J. Phys.: Condens. Matter **17** (2005) 8017–8028 doi:10.1088/0953-8984/17/50/019

Multiple-scattering effects in Ga K-edge extended x-ray absorption fine structure spectra of GaP, GaAs and GaSb semiconductor compounds

Shiqiang Wei[1] **and Zhihu Sun**

National Synchrotron Radiation Laboratory, University of Science and Technology of China, Hefei, Anhui 230029, People's Republic of China

E-mail: sqwei@ustc.edu.cn

Received 30 September 2005, in final form 3 October 2005
Published 2 December 2005
Online at stacks.iop.org/JPhysCM/17/8017

Abstract

The dependence of Ga K-edge multiple-scattering extended x-ray absorption fine structure (MS-EXAFS) effects on the nearest neighbours in GaP, GaAs and GaSb semiconductor compounds with the zinc blende structure has been comprehensively investigated by considering the coordination environment within the first three shells around the Ga atoms. It is revealed that in the case of GaP with a light element as the first neighbour of the Ga absorber, the MS-EXAFS effects are negligibly weak with respect to the single-scattering (SS) contribution. For GaAs and GaSb compounds with heavier elements as the first neighbour of the Ga absorber, the MS effects become increasingly important and are dominated by a triangular double-scattering path DS2 ($Ga_0 \rightarrow B_1 \rightarrow B_2 \rightarrow Ga_0$). The EXAFS contribution of the DS2 path destructively interferes with that of the second shell single-scattering path (SS2), with the amplitude ratio of DS2 to SS2 rising from 7% for GaP to 25 and 70% for GaAs and GaSb, respectively. This indicates that the second shell peak magnitude for these compounds is increasingly damped by the MS effects as the first nearest neighbour goes from P to Sb. Based on these results, we present a generalized and simplified high-shell MS-EXAFS analysis method for compounds with the open structure of zinc blende.

1. Introduction

In the last decade, low-dimensional III–V semiconductors such as quantum dots [1, 2] and wells [3, 4] have attracted a wide research interest due to their excellent optical and optoelectronic performances that make them promising candidates for fabricating infrared lasers and light-emitters in the long wavelength (1.3–1.6 μm) region [5, 6]. The local lattice in

[1] Author to whom any correspondence should be addressed.

these low-dimensional systems is inevitably distorted with respect to their bulk counterparts. As a result, this distortion significantly modifies the electronic and optical properties of the low-dimensional semiconductors. In addition, theoretical calculations of electronic and optical properties of the low-dimensional semiconductors also require direct information on their structural parameters, not only in crystallographic average, but also in local structural viewpoints. Therefore, the understanding of their atomic structure parameters is of crucial importance for these low-dimensional systems [7, 8].

The x-ray absorption fine structure (XAFS) technique has been recognized as a powerful tool for determining the local structure of condensed matter because of its sensitivity to the short-range order and atomic species surrounding the absorbing atom. A series of XAFS studies has demonstrated that the structural information of the first shell in the III–V semiconductors can be easily and reliably obtained by means of extended x-ray absorption fine structure (EXAFS) in the framework of the single-scattering (SS) approximation [9–12]. However, as far as the local structures beyond the first shell are concerned, the EXAFS analysis becomes much more complicated and challenging because of the numerous multiple-scattering (MS) processes of the emitted photoelectrons. There exists a discrepancy in the treatment of the MS EXAFS effects for the III–V semiconductors. For example, for the strained $In_xGa_{1-x}As/GaAs$ heterostructures [13] the MS contributions within the second and third shells were simply neglected, while for the $In_xGa_{1-x}As/InP$ [14], $GaAs_{1-x}P_x/GaAs$ [15] epitaxial films and $InAs_xP_{1-x}/InP$ superlattices [16] the MS effects were apparently taken into account and proved to be essential in obtaining the interatomic distances of the second and third shells. Hence, a detailed study on the MS effects of the zinc blende structured III–V semiconductors is required.

The MS effects are strongly dependent on the scattering path geometry and the atom species involved in the scattering events [17]. All the III–V semiconductors with zinc blende structure have the same scattering path arrangements. It may be expected that they should have the same shape in their radial structural functions (RSFs). However, as shown in figure 3, the RSFs around Ga atoms for GaP, GaAs and GaSb crystals exhibit significantly different features, especially in the second shell. This difference demonstrates that the first nearest neighbour of the Ga atoms has a distinguishable impact on the second peak, depending on the nearest neighbour being P, As or Sb atoms. This impact can only be possible via the MS processes involving the first nearest neighbour. Therefore it is of interest to know how the MS effects are influenced by the different scattering atomic species. Moreover, this can also be helpful in simplifying the MS analysis by neglecting the unimportant scattering paths.

In this work, we will perform a detailed study on the MS-EXAFS processes of the crystalline GaM (M = P, As, Sb) semiconductor compounds with zinc blende structure. The P, As and Sb are elements in the third, fourth and fifth row of the Periodic Table, respectively, having distinct scattering characteristics to the photoelectrons. Therefore the GaP, GaAs and GaSb crystals are good model compounds for a comparative study of the MS effects in the III–V semiconductors. Our aims are to study the dependence of the MS effects on P, As and Sb neighbours, and then propose a simplified and effective MS-EXAFS analysis method for all the semiconductor compounds with the zinc blende structure.

2. Experiment

The crystalline GaP, GaAs and GaSb samples for XAFS measurement were prepared as follows. Fine powder with grain size of about 20 μm prepared from its single crystal was homogeneously mixed with BN powder. Then the mixed powder was pressed into tablets with the diameter of 10 mm and thickness of 0.5 mm. The ratio of GaP (GaAs and GaSb) to BN powder was optimized by making the absorption jump $\Delta\mu x \approx 1$ at its Ga K-edge.

Table 1. The denotation and degeneracy of paths used in the fits. In the left-hand column, Ga_0 is the central absorber atom. B_1, B_2 and B_3 identify scattering atoms in the first, second and third shell, respectively. B_1' denotes an atom in the first shell different from atom B_1.

Path	Denotation	Degeneracy
$Ga_0 \rightarrow B_1 \rightarrow Ga_0$	SS1	4
$Ga_0 \rightarrow B_2 \rightarrow Ga_0$	SS2	12
$Ga_0 \rightarrow B_3 \rightarrow Ga_0$	SS3	12
$Ga_0 \rightarrow B_1 \rightarrow B_1' \rightarrow Ga_0$	DS1	12
$Ga_0 \rightarrow B_1 \rightarrow B_2 \rightarrow Ga_0$	DS2	24
$Ga_0 \rightarrow B_1' \rightarrow B_2 \rightarrow Ga_0$	DS3	48
$Ga_0 \rightarrow B_1 \rightarrow B_3 \rightarrow Ga_0$	DS4	48
$Ga_0 \rightarrow B_2 \rightarrow B_3 \rightarrow Ga_0$	DS5	48
$Ga_0 \rightarrow B_1 \rightarrow Ga_0 \rightarrow B_1 \rightarrow Ga_0$	TS1	4
$Ga_0 \rightarrow B_1 \rightarrow B_2 \rightarrow B_1 \rightarrow Ga_0$	TS2	12

The Ga K-edge XAFS measurements of GaP, GaAs and GaSb powders were performed at the BL-13B beamline of the Photon Factory, National Laboratory for High Energy Physics (PF, KEK), and at the beamline of U7C of National Synchrotron Radiation Laboratory (NSRL). The electron beam energy of the Photon Factory was 2.5 GeV and the maximum stored current was 400 mA. A 27-pole wiggler with the maximum magnetic field of 1.5 T inserted in the straight section of the storage ring was used [18]. The storage ring of the NSRL was operated at 0.8 GeV with a maximum current of 300 mA. The hard x-ray beam was from a 3-pole superconducting wiggler with a magnetic field intensity of 6 T [19]. Fixed-exit Si(111) flat double crystals were used as the monochromator. The energy resolution was about 2–3 eV by using the Cu foil 3d near K-edge feature. The x-ray harmonics were minimized by detuning the two flat Si(111) crystal monochromators to about 70% of the maximum incident light intensity. Ionization chambers filled with Ar/N_2 mixed gases were used to collect the XAFS spectra in transmission mode at room temperature.

3. Data analysis

The EXAFS $\chi(k)$ functions of GaP, GaAs and GaSb powders were obtained by using NSRL-XAFS3.0 software package [20] according to the standard procedures, and the fits to the spectra were done in R-space by using the FEFFIT code of UWXAFS3.0 package [21]. The theoretical amplitudes and phase-shifts of all the scattering processes within the first three shells were yielded from the FEFF7 [22] calculation, which was performed from the known crystallographic structure of zinc blende. The lattice constants used for the calculations were 5.450, 5.654 and 6.095 Å for GaP, GaAs and GaSb, respectively. By selecting those paths whose amplitude has a weight greater than 3% of the largest one, we obtained ten pronounced scattering paths within the first three shells. The path denotations and degeneracies are listed in table 1, and the arrangement of some scattering paths is schematically shown in figure 1.

In the curve-fitting procedure, the coordination numbers are fixed to the nominal values of the paths. The following parameters of each path are either fixed or allowed to vary: interatomic distance R, passive electron reduction factor S_0^2, shift of the energy origin ΔE_0, Debye–Waller factor σ^2 and the third cumulant $\sigma^{(3)}$. The interatomic distance R is assumed to relate to changes in the lattice constant Δa, which decreases the number of independent parameters to be one for all paths. The S_0^2 is first treated as an adjustable variable in the first-shell fitting for all three compounds. The obtained results of S_0^2 were 0.98, 1.0 and 0.86 for GaP, GaAs and

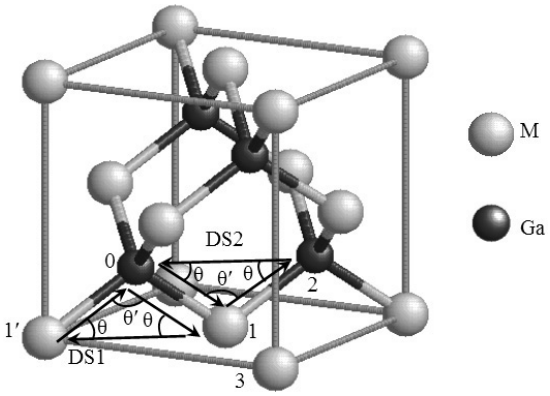

Figure 1. The zinc blende structure of crystalline GaM (M = P, As and Sb) with the representative Ga and M atoms in the first three shells. The number 0 refers to the central absorber Ga atom. Numbers 1–3 identify corresponding coordination shell atoms and number 1′ denotes another first coordination shell atom different from atom 1. Two different DS paths DS1 and DS2 are also described.

GaSb respectively. Then for each compound the S_0^2 value was fixed to be the obtained value for all subsequent MS analyses.

Three independent Debye–Waller factors σ^2 are assigned to three SS paths as adjustable variables. For the MS paths, the σ^2 are assumed to be not totally independent. For example, it is a reasonable approximation to assume that the corresponding double scattering (DS) paths with the same half path lengths have equal Debye–Waller factors [17]. For the TS paths $Ga_0 \rightarrow B_1 \rightarrow Ga_0 \rightarrow B_1 \rightarrow Ga_0$ and $Ga_0 \rightarrow B_1 \rightarrow B_2 \rightarrow B_1 \rightarrow Ga_0$ it is also reasonable to set their Debye–Waller factors to be twice the value σ_1^2 of the first shell [17]. The third cumulant $\sigma^{(3)}$ is also included in the fits to take into account the asymmetry of distance distributions. Since the absorber atom Ga in these compounds is electronically charged, the approximation of neutral absorber atom assumed by FEFF7 is not valid. In order to compensate for this effect, it is necessary to add an additional ΔE_0 to all those MS paths involving scattering from the first nearest neighbour. The physical reason is that if the core hole potential is not well shielded, it will strongly perturb the potential at its first neighbour site from approximate spherical symmetry [23]. Besides, for all other SS or MS paths not involving the first nearest neighbour, a common variable ΔE_0 is assigned.

4. Results and discussion

The k^2-weighted $\chi(k)$ curves of GaP, GaAs and GaSb compounds are shown in figure 2. The oscillation magnitude of GaP is the strongest at 4–6 $Å^{-1}$ but it decreases very quickly. The spectrum of GaAs shows a maximum oscillation at 7–9 $Å^{-1}$. For GaSb, its spectrum presents two maxima at 4 and 9 $Å^{-1}$, respectively. The different features of the EXAFS spectra of GaP, GaAs and GaSb reflect the distinct scattering characteristics of P, As and Sb atoms to the photoelectron wave emitted from the absorbing Ga atoms. This obvious difference is further exhibited in figure 3, where the solid lines show the radial structural functions (RSFs) by Fourier transforming the experimental $k^2\chi(k)$ spectra in the k-range from 3 to 16 $Å^{-1}$. Although in all these compounds Ga atoms are coordinated by 12 Ga atoms as the second nearest neighbours, the peak intensities associated with second and third shells are damped very quickly with the nearest neighbour going from P to Sb. The second and third peaks of

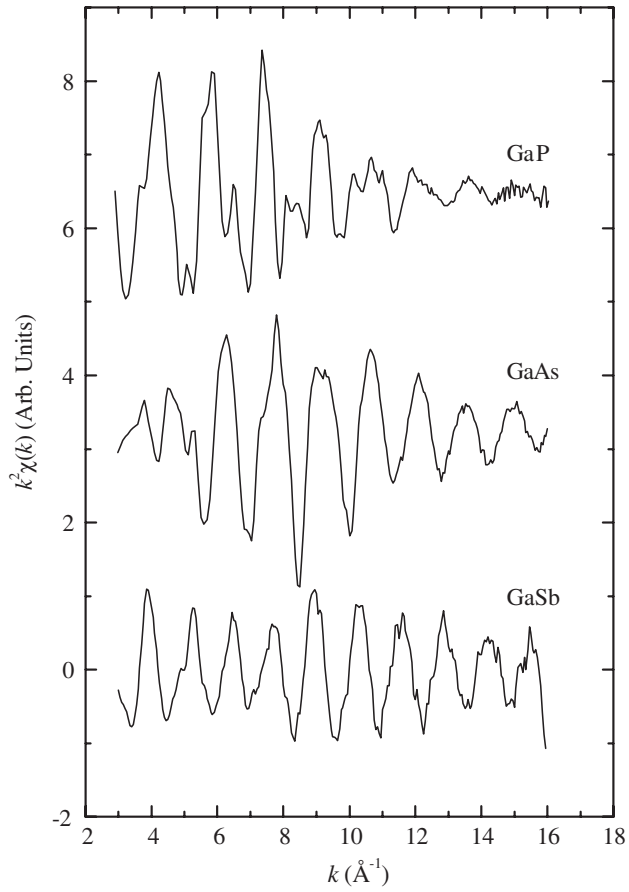

Figure 2. $k^2\chi(k)$ EXAFS oscillation functions recorded at the Ga K-edge for crystalline GaP, GaAs and GaSb.

GaP are overlapped; their heights are about 40% and 25% of that of the first peak, respectively. For GaAs, the peaks related to the first three shells are well separated. The intensities of the second and third peak drop to about 25% and 15% of that of the first peak. In the case of GaSb, the higher shell peaks are difficult to distinguish because of their weak intensities.

The curve-fitting results in R-space are shown in figure 3 as circles. The fits were done in the intervals including the first three peaks, namely, [1.0, 4.6], [1.2, 4.8], and [1.5, 5.4] Å for GaP, GaAs and GaSb, respectively. The obtained path parameters of various SS and MS paths for these compounds are presented in tables 2–4, where the fitting reliability factors $\mathcal{R}$ are also listed. Here $\mathcal{R}$ is defined as

$$\mathcal{R} = \frac{\sum_i [|\chi_{\rm exp}(R_i) - \chi_{\rm fit}(R_i)|]^2}{\sum_i |\chi_{\rm exp}(R_i)|^2}. \tag{1}$$

The $\mathcal{R}$ values for all three compounds are below 0.005, indicating that the experimental spectra are well reproduced by the fits. The determination of error bars is consistent with the criteria adopted by the International XAFS Society [24], i.e., the error bars are estimated from the square root of the diagonal elements of the correlation matrix.

In order to distinguish the contributions of various scattering paths to the EXAFS spectra of GaP, GaAs and GaSb, we plot their oscillation curves in k-space and amplitude peaks in

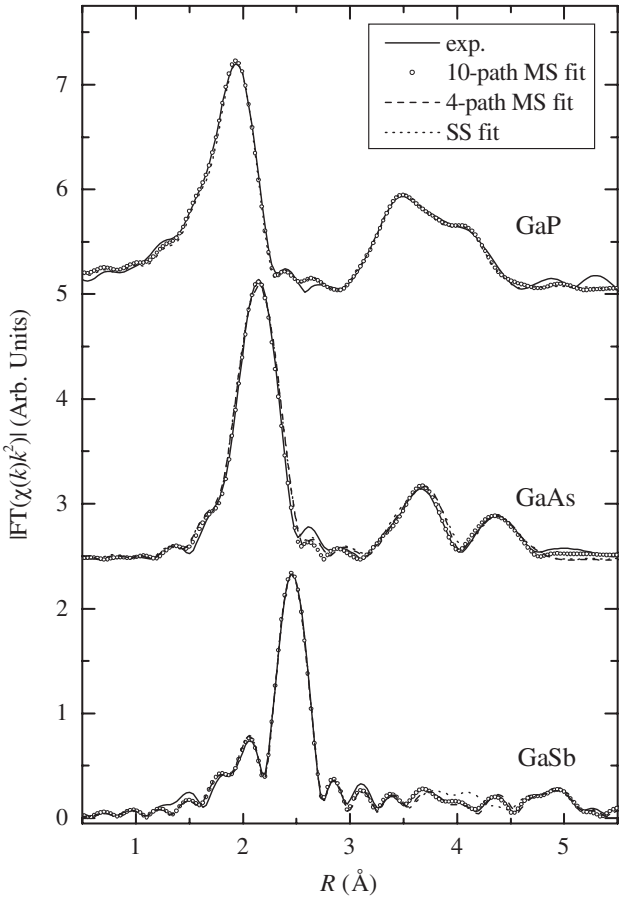

Figure 3. The radial structural function (RSF) by Fourier transforming $k^2\chi(k)$ for crystalline GaP, GaAs and GaSb: experiment (solid line), MS fit including ten paths (circle), MS fit including four paths (dashed line) and SS fit (dotted line).

R-space in figures 4 and 5, respectively. Three striking features can be observed from these figures. First, all the MS paths of GaP contribute quite weak EXAFS signals as compared with its SS paths, but the MS path $Ga_0 \rightarrow B_1 \rightarrow B_2 \rightarrow Ga_0$ (DS2) of GaAs and GaSb provides comparable EXAFS contribution relative to those of their SS paths. Second, the oscillations of DS2 and the single-scattering path of the second shell (SS2) are opposite in phase, implying the destructive interference between their EXAFS oscillations. Third, the EXAFS oscillation amplitude of DS2 path rapidly increases with the nearest neighbour going from P to Sb atom. The amplitude ratio of DS2 to SS2 is only 7% for GaP, and then rises to about 25% and 70% for GaAs and GaSb, respectively. Since the DS2 and SS2 paths have close values of Debye–Waller factor in the same crystal, as shown in tables 2–4, the variation in the amplitude ratio of DS2/SS2 can only be attributed to the different scattering characteristics of the intervening atoms. Since the R-space peak position of DS2 is close to that of SS2, their increasingly stronger destructive interference from GaP, GaAs to GaSb explains the observed difference in the RSFs of these compounds well.

The above discussions lead us to conclude that the SS approximation is sufficient in analysing the EXAFS spectrum of GaP, and that only the contributions of SS paths plus

Table 2. Path parameters and reliability factor $\mathcal{R}$ obtained from a multiple-scattering fit by using ten paths for GaP. The parameters in parentheses are obtained by including only SS paths.

Path	R (Å)	σ^2 (10^{-3} Å^2)	$\sigma^{(3)}$ (10^{-4} Å^3)	ΔE_0 (eV)	Δa (Å)	$\mathcal{R}$
SS1	2.363 ± 0.010	4.2 ± 0.1	1.1 ± 1.3	7.0 ± 1.0	0.008 ± 0.022	0.0026
	(2.364 ± 0.010)	(4.1 ± 0.1)	(1.5 ± 1.0)	(5.5 ± 0.6)	(0.010 ± 0.018)	(0.0039)
SS2	3.859 ± 0.017	9.2 ± 0.4	1.9 ± 3.4	6.5 ± 1.5		
	(3.860 ± 0.016)	(9.4 ± 0.3)	(3.0 ± 2.0)	(5.2 ± 1.1)		
SS3	4.525 ± 0.020	10.9 ± 1.2	4.6 ± 6.0	6.5 ± 1.5		
	(4.527 ± 0.018)	(10.6 ± 1.0)	(5.0 ± 6.0)	(5.2 ± 1.1)		
DS1	4.293 ± 0.020	8.5 ± 1.3	4.6 ± 6.0	5.9 ± 1.4		
DS2	4.293 ± 0.020	8.5 ± 1.3	4.6 ± 6.0	5.9 ± 1.4		
DS3	5.374 ± 0.024	12.7 ± 4.0	4.6 ± 6.0	5.9 ± 1.4		
DS4	5.374 ± 0.024	12.7 ± 4.0	4.6 ± 6.0	5.9 ± 1.4		
DS5	5.374 ± 0.024	12.7 ± 4.0	4.6 ± 6.0	6.5 ± 1.5		
TS1	4.726 ± 0.022	8.5 ± 0.4	4.6 ± 6.0	5.9 ± 1.4		
TS2	4.726 ± 0.022	8.5 ± 0.4	4.6 ± 6.0	5.9 ± 1.4		

Table 3. Path parameters and reliability factor $\mathcal{R}$ obtained from a multiple-scattering fit by using ten paths for GaAs. The parameters in parentheses and square brackets are obtained by including four paths (SS plus DS2) and only SS paths, respectively.

Path	R (Å)	σ^2 (10^{-3} Å^2)	$\sigma^{(3)}$ (10^{-4} Å^3)	ΔE_0 (eV)	Δa (Å)	$\mathcal{R}$
SSI	2.458 ± 0.010	4.5 ± 0.1	1.0 ± 0.9	3.4 ± 1.5	0.022 ± 0.040	0.0036
	(2.455 ± 0.008)	(4.5 ± 0.1)	(0.8 ± 1.0)	(4.4 ± 1.5)	(0.015 ± 0.030)	(0.0053)
	$[2.455 \pm 0.009]$	$[4.5 \pm 0.1]$	$[0.8 \pm 0.8]$	$[4.3 \pm 1.2]$	$[0.014 \pm 0.035]$	[0.0079]
SS2	4.014 ± 0.016	11.8 ± 0.9	0.0 ± 2.8	4.0 ± 1.3		
	(4.009 ± 0.012)	(11.4 ± 0.6)	(0.9 ± 2.5)	(4.8 ± 1.8)		
	$[4.009 \pm 0.014]$	$[13.2 \pm 0.7]$	$[2.1 \pm 4.0]$	$[5.0 \pm 2.0]$		
SS3	4.707 ± 0.019	13.2 ± 1.0	0.6 ± 4.0	4.0 ± 1.3		
	(4.700 ± 0.015)	(13.6 ± 1.1)	(1.1 ± 5.0)	(4.5 ± 2.3)		
	$[4.700 \pm 0.017]$	$[13.9 \pm 1.6]$	$[2.0 \pm 5.4]$	$[5.0 \pm 2.0]$		
DS1	4.465 ± 0.018	10.8 ± 5.2	0.6 ± 4.0	7.7 ± 2.4		
DS2	4.465 ± 0.018	10.8 ± 5.2	0.6 ± 4.0	7.7 ± 2.4		
	(4.459 ± 0.014)	(11.2 ± 5.6)	(1.1 ± 5.0)	(6.4 ± 2.6)		
DS3	5.589 ± 0.023	10.6 ± 10.1	0.6 ± 4.0	7.7 ± 2.4		
DS4	5.589 ± 0.023	10.6 ± 10.1	0.6 ± 4.0	7.7 ± 2.4		
DS5	5.589 ± 0.023	10.6 ± 10.1	0.6 ± 4.0	4.0 ± 1.3		
TS1	4.916 ± 0.020	9.0 ± 0.2	0.6 ± 4.0	7.7 ± 2.4		
TS2	4.916 ± 0.020	9.0 ± 0.2	0.6 ± 4.0	7.7 ± 2.4		

DS2 should be included in analysing the higher shell local structures of GaAs and GaSb. This conclusion is confirmed by the curve-fitting results demonstrated in figure 3 as dashed lines as well as by the obtained structural parameters and $\mathcal{R}$ factor presented in tables 2–4 in parentheses. The values of $\mathcal{R}$ factors increase slightly in these simplified fittings, but are all below 0.006, indicating that the fitting quality is still quite good. Within error bars the structural parameters are almost the same as those obtained from considering all the ten scattering paths.

Although for GaAs and GaSb the DS2 path contributes comparable EXAFS signals to those of SS2, it may be doubtful if their DS2 paths' contributions can also be neglected just like in the case of GaP. In figure 3 the SS fits are compared with the ten-path MS fits for GaAs and GaSb. The extracted structural parameters and $\mathcal{R}$ factors are listed in tables 3 and 4 in square brackets. It can be seen that for GaAs, the SS fitting quality is still acceptable, while the

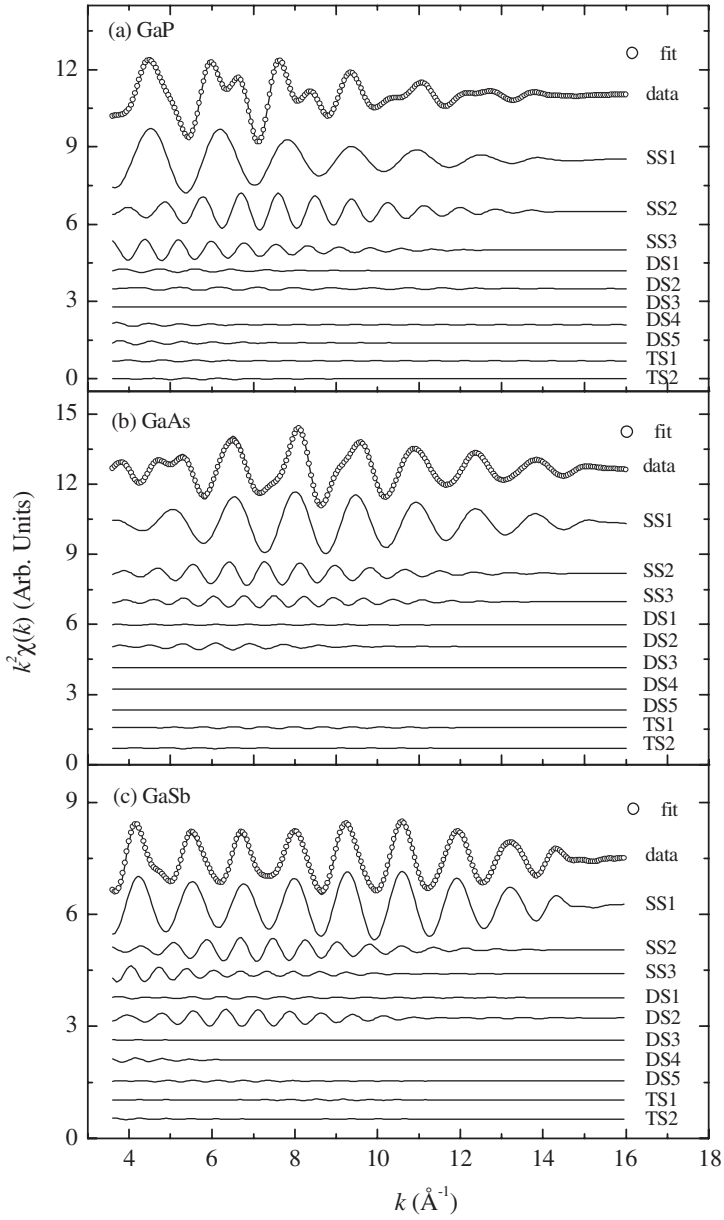

Figure 4. Contributions of the individual scattering paths to the total EXAFS oscillation function $k^2\chi(k)$ for crystalline (a) GaP, (b) GaAs, and (c) GaSb.

second shell Debye–Waller factor σ_2^2 is a little overestimated. However, for GaSb, the SS fit cannot reproduce the experimental features in the R-range from 3.5 to 4.5 Å, and the obtained σ_2^2 is obviously too large. The increased σ_2^2 in the SS fits is a natural result of neglecting DS2, since SS2 has to excessively lower its amplitude to compensate for the amplitude damping due to the destructive interference between the oscillations of DS2 and SS2 paths.

The MS-EXAFS effects of GaAs have been previously investigated by Dalba *et al* using the fast spherical approximation [25]. The dependence of the MS contribution on the bonding

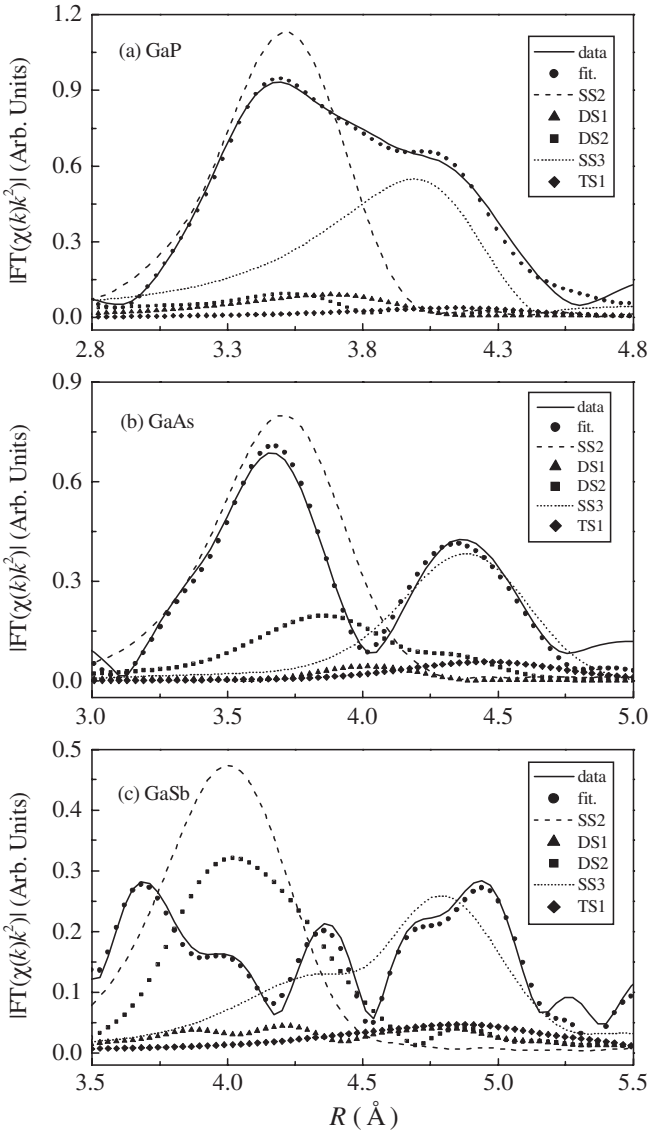

Figure 5. Contributions of the scattering paths to the RSFs of the second and third shell peaks for crystalline (a) GaP, (b) GaAs, and (c) GaSb.

angle Ga_0–As_1–Ga_2 was calculated, which corresponds to the DS2 path in this work. By comparing the EXAFS amplitude of DS2 path with that of SS2 path, the authors concluded that the MS contribution was negligible for the angle Ga_0–As_1–Ga_2 below 135°, and only the angle above 155° could lead to a considerable increase of the EXAFS amplitude. Since in the real crystal structure of zinc blende this angle is 109.5°, it was claimed that MS contributions generated within the first and second shells could be neglected for crystalline compounds with the open structure of zinc blende. In fact, our MS-EXAFS results show that the MS effects in open structures strongly depend on the atomic species of the nearest neighbour. As can be seen from figures 4 and 5, the amplitude of MS contributions experiences a drastic change from

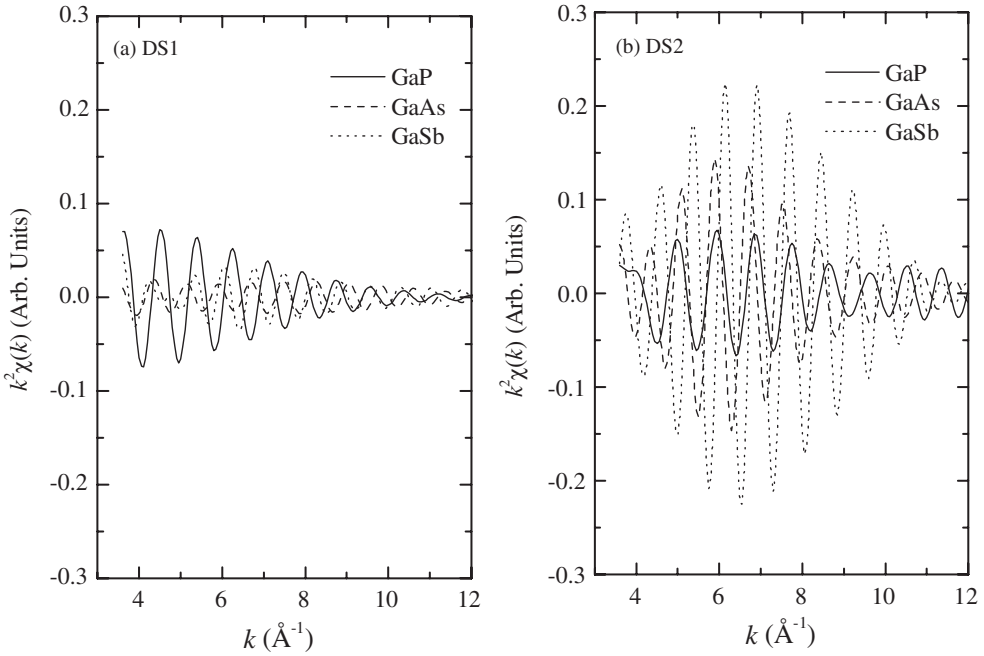

Figure 6. Comparison of EXAFS oscillations of DS1 and DS2 paths in GaP, GaAs and GaSb.

Table 4. Path parameters and reliability factor $\mathcal{R}$ obtained from a multiple-scattering fit by using ten paths for GaSb. The parameters in parentheses and square brackets are obtained by including four paths (SS plus DS2) and only SS paths, respectively.

Path	R (Å)	σ^2 (10^{-3} Å^2)	$\sigma^{(3)}$ (10^{-4} Å^3)	ΔE_0 (eV)	Δa (Å)	$\mathcal{R}$
SS1	2.639 ± 0.005	4.9 ± 0.1	-1.3 ± 0.5	2.9 ± 0.3	-0.001 ± 0.007	0.0039
	(2.638 ± 0.007)	(4.9 ± 0.1)	(-1.2 ± 0.6)	(2.4 ± 0.5)	(-0.002 ± 0.010)	(0.0057)
	$[2.640 \pm 0.007]$	$[4.9 \pm 0.1]$	$[-1.1 \pm 0.9]$	$[2.6 \pm 0.6]$	$[0.001 \pm 0.010]$	[0.018]
SS2	4.310 ± 0.007	13.5 ± 1.1	-3.5 ± 1.5	4.1 ± 0.7		
	(4.309 ± 0.010)	(12.7 ± 1.7)	(-4.0 ± 2.0)	(3.2 ± 0.7)		
	$[4.311 \pm 0.010]$	$[16.1 \pm 5.0]$	$[-2.6 \pm 1.3]$	$[2.5 \pm 1.1]$		
SS3	5.054 ± 0.008	17.3 ± 3.6	-1.5 ± 2.0	4.1 ± 0.7		
	(5.053 ± 0.012)	(18.0 ± 3.0)	(-1.0 ± 2.0)	(3.2 ± 0.7)		
	(5.055 ± 0.012)	$[17.6 \pm 3.3]$	$[-0.7 \pm 2.0]$	$[2.5 \pm 1.1]$		
DS1	4.794 ± 0.008	10.5 ± 1.7	-1.5 ± 2.0	2.6 ± 0.9		
DS2	4.794 ± 0.008	10.5 ± 1.7	-1.5 ± 2.0	2.6 ± 0.9		
	(4.793 ± 0.012)	(10.0 ± 2.1)	(-1.0 ± 2.0)	(2.1 ± 1.2)		
DS3	6.001 ± 0.010	19.2 ± 9.7	-1.5 ± 2.0	2.6 ± 0.9		
DS4	6.001 ± 0.010	19.2 ± 9.7	-1.5 ± 2.0	2.6 ± 0.9		
DS5	6.001 ± 0.010	19.2 ± 9.7	-1.5 ± 2.0	4.1 ± 0.7		
TS1	5.278 ± 0.009	9.2 ± 0.2	-1.5 ± 2.0	2.6 ± 0.9		
TS2	5.278 ± 0.009	9.2 ± 0.2	-1.5 ± 2.0	2.6 ± 0.9		

GaP to GaSb. For a light scattering element like P as the nearest neighbour, the MS effects are indeed negligible; for a medium element like As, the MS contributions are reasonably strong; while for a heavy element like Sb, the MS processes occurring in the first and second shells make significantly strong contributions to the total EXAFS spectrum.

We have seen that the nearest neighbours of Ga atoms play a critical role in determining the MS-EXAFS contributions. However, it should be remarked that the significance of the MS effects also depends on the scattering path configuration. As an example, let us compare the MS contributions of two DS paths with the same scattering path length, i.e., DS1 ($Ga_0 \rightarrow B_1 \rightarrow B_1' \rightarrow Ga_0$) and DS2 in a Ga–M (M = P, As, Sb) compound. The DS1 scattering occurs within the tetrahedron formed by the first nearest neighbour M atoms, while DS2 scattering involves the first nearest neighbour M and the second nearest neighbour Ga atoms as the scatterers. Figure 6 displays that in GaP the EXAFS amplitude of DS1 is similar to that of DS2, while in GaAs and GaSb the latter is much stronger than the former. The configuration-dependent contributions of DS paths can be easily understood from the formula proposed by Lee and Pendry [26], which depicts the oscillation function $\chi(k)$ of a DS path with two scatterers at $\vec{R}_1$ and $\vec{R}_2$ to be

$$\chi(k) \propto f(k,\theta_1) f(k,\theta_2) \frac{e^{ik(R_1+|\vec{R}_2-\vec{R}_1|+R_2)}}{kR_1|\vec{R}_2-\vec{R}_1|R_2}. \tag{2}$$

Here θ_1 is the angle between $\vec{R}_1$ and $\vec{R}_2-\vec{R}_1$, θ_2 is that between $\vec{R}_2-\vec{R}_1$ and $-\vec{R}_2$, and $f(k,\theta)$ is the scattering amplitude:

$$f(k,\theta) = \frac{1}{k}\sum_{l=0}^{\infty}(2l+1)e^{i\delta_l}\sin\delta_l P_l(\cos\theta). \tag{3}$$

As is seen from tables 2–4, the DS1 and DS2 paths in the same compound Ga–M (M = P, As, Sb) have equal path length and Debye–Waller factor. Therefore, the difference between the oscillation functions $\chi(k)$ of the DS1 and DS2 paths in Ga–M (M = P, As, Sb) comes from the different scattering amplitudes of the intervening atoms at the scattering angles 144.7° and 70.5°, i.e., $\chi_{DS1}(k) \propto f_M(k, 144.7°) f_M(k, 144.7°)$, $\chi_{DS2}(k) \propto f_M(k, 70.5°) f_{Ga}(k, 144.7°)$.

The noncollinear MS processes have also been previously studied for other tetrahedrally coordinated systems such as $KMnO_4$, [27, 28] $GeCl_4$, GeH_3Cl and GeH_4 [29], as well as K_2CrO_4 compounds [30]. These works focused on the MS paths within the tetrahedron formed by the first nearest neighbours just like DS1 in this work. It was suggested that the contribution of DS1 was important in the XANES region [27–29], while it was unimportant in the EXAFS region when the bond lengths were larger than 1.6 Å [27]. Our work also shows that for the tetrahedrally coordinated III–V compounds, the noncollinear MS processes in the first shell contribute insignificant signals to the total EXAFS spectrum even in the case of GaP with the strongest EXAFS intensity of DS1.

Based on the above results on GaP, GaAs and GaSb compounds, we can present a simplified MS-EXAFS data analysis method for compounds with zinc blende and diamond structures. For a compound with light elements such as Si, P, S, N, O as the nearest neighbour of the absorbing atoms, the MS effects are negligible and the SS approximation is sufficient in analysing their local structures within the third shell. In a case where the nearest neighbour is a medium heavy atom like Ga, Ge and As, it is accurate enough to consider only the contribution of the DS2 path as the MS effect. If a heavier atom like In (or Sn, Sb) is the nearest neighbour, the contribution of the DS2 path is very strong and it must be included in analysing the higher shell local structures.

5. Conclusion

A detailed MS-EXAFS analysis has been performed on the local structure around Ga atoms up to the third shell for crystalline GaM (M = P, As, Sb) compounds. Three SS paths and seven MS paths were used to fit the EXAFS spectra. In these compounds the MS effects

within the first three coordination shells are strongly dependent on the atomic species of the nearest neighbours. The MS effects of GaAs and GaSb are dominated by the double-scattering path DS2, but the MS contribution of GaP is negligible. The EXAFS signal of the DS2 path destructively interferes with that of the single-scattering path (SS2) of the second shell and therefore reduces the peak intensity of the latter in R-space. The EXAFS amplitude ratio of DS2 to SS2 is about 70%, 25% and 7% for GaSb, GaAs and GaP, respectively. Besides the forward-scattering power of the neighbouring atoms, the geometrical arrangement of the scattering paths is also shown to play an important role in determining the noncollinear MS effects. Summarizing these results on GaM (M = P, As, Sb) compounds, we propose a simplified MS-EXAFS data analysis method for semiconductor compounds with zinc blende and diamond structures.

Acknowledgments

This work was supported by the National Science Foundation of China (Grant No. 10375059 and 10174068), Acknowledge Innovation program of Chinese Academy of Sciences, and Specialized Research Fund for the Doctoral Program of Higher Education. The authors are grateful for useful discussions about this work with Professor H Oyanagi.

References

[1] Le Ru E C, Howe P, Jones T S and Murray R 2003 *Phys. Rev.* B **67** 165303
[2] Mazur Y I, Wang Z M, Tarasov G G, Xiao M, Salamo G J, Tomm J W, Talalaev V and Kissel H 2005 *Appl. Phys. Lett.* **86** 063102
[3] Li L H, Sallet V, Patriarche G, Largeau L, Bouchoule S, Travers L and Harmand J C 2003 *Appl. Phys. Lett.* **83** 1298
[4] Wang S M, Zhao Q X, Wang X D, Wei Y Q, Sadeghi M and Larsson A 2005 *Appl. Phys. Lett.* **85** 875
[5] Grundmann M 2000 *Physica* E **5** 167
[6] Tångring I, Wang S M, Gu Q F, Wei Y Q, Sadeghi M, Larsson A, Zhao Q X, Akram M N and Berggren J 2005 *Appl. Phys. Lett.* **86** 171902
[7] Kim K and Zunger A 2001 *Phys. Rev. Lett.* **86** 2609
[8] Lordi V, Gambin V, Friedrich S, Funk T, Takizawa T, Uno K and Harris J S 2003 *Phys. Rev. Lett.* **90** 145505
[9] Boscherini F, Lamberti C, Pascarelli S, Rigo C and Mobilio S 1998 *Phys. Rev.* B **58** 10745
[10] Romanato F, De Salvador D, Berti M, Drigo A, Natali M, Torman M, Rossetto G, Pascarelli S, Boscherini F, Lamberti C and Mobilio S 1998 *Phys. Rev.* B **57** 14619
[11] Proietti M, Renevier H, Hodeau J, Garcia J, Bérar J and Wolfers P 1999 *Phys. Rev.* B **59** 5479
[12] d'Acapito F, Boscherini F, Mobilio S, Rizzi A and Lantier R 2002 *Phys. Rev.* B **66** 205411
[13] Proietti M G, Turchini S, Garcia J, Lamble G, Martelli F and Prosperi T 1995 *J. Appl. Phys.* **78** 6574
[14] Tormen M, De Salvador D, Drigo A V, Romanato F, Boscherini F and Mobilio S 2001 *Phys. Rev.* B **63** 115326
[15] Proietti M G, Renevier H, Hodeau J L, García J, Bérar J F and Wolfers P 1999 *Phys. Rev.* B **59** 5479
[16] Pascarelli S, Boscherini F, Lamberti C and Mobilio S 1997 *Phys. Rev.* B **56** 1936
[17] Frenkel A I, Stern E A, Qian M and Newville M 1993 *Phys. Rev.* B **48** 12449
[18] Oyanagi H, Owen I, Grimshaw M, Head P, Martini M and Saito M 1995 *Rev. Sci. Instrum.* **66** 5477
[19] Xu F Q, Liu W H, Wei S Q, Xu C Y, Pan G Q, Zhang X Y, Sun J W, Zhao W C, Cui H and B and Ye W Q 2001 *J. Synchrotron Radiat.* **8** 348
[20] Zhong W J and Wei S Q 2001 *J. Univ. Sci. Technol. China* **31** 328
[21] Stern E A, Newville M, Ravel B, Yakoby Y and Haskel D 1995 *Physica* B **208/209** 117
[22] Ankudinov A L and Rehr J J 1997 *Phys. Rev.* B **56** R1712
[23] Haskel D, Ravel B, Newville M and Stern E A 1995 *Physica* B **208/209** 151
[24] Lytle F W, Sayers D E and Stern E A 1989 *Physica* B **158** 701
[25] Dalba G, Diop D, Fornasini P, Kuzmin A and Rocca F 1993 *J. Phys.: Condens. Matter* **5** 1643
[26] Lee P A and Pendry J P 1975 *Phys. Rev.* B **11** 2795
[27] Bunker G and Stern E 1984 *Phys. Rev. Lett.* **52** 1990
[28] Benfatto M, Natoli C R, Bianconi A, Garcia J, Marcelli A, Fanfoni M and Davoli I 1986 *Phys. Rev.* B **34** 5774
[29] Bouldin C E, Bunker G, McKeown D A, Forman R A and Ritter J J 1988 *Phys. Rev.* B **38** 10816
[30] Pandya K I 1994 *Phys. Rev.* B **50** 15509